Osteoarthritis and Cartilage 22 (2014) 1488–1498

Osteoarthritis and Cartilage

Severity mapping of the proximal femur: a new method for assessing hip osteoarthritis with computed tomography

T.D. Turmezei †‡§*, D.J. Lomas ‡, M.A. Hopper ‡, K.E.S. Poole §

† Department of Engineering, University of Cambridge, Trumpington Street, Cambridge CB2 1PZ, UK
‡ Department of Radiology, Box 218, Level 5, Addenbrooke's Hospital, Hills Road, Cambridge CB2 0QQ, UK
§ Department of Medicine, Box 157, Level 5, Addenbrooke's Hospital, Hills Road, Cambridge CB2 0QQ, UK

ARTICLE INFO

Article history:
Received 3 January 2014
Accepted 4 March 2014

Keywords:
Osteoarthritis
Hip joint
Computed tomography
Phenotyping

SUMMARY

Objective: Plain radiography has been the mainstay of imaging assessment in osteoarthritis for over 50 years, but it does have limitations. Here we present the methodology and results of a new technique for identifying, grading, and mapping the severity and spatial distribution of osteoarthritic disease features at the hip in 3D with clinical computed tomography (CT).

Design: CT imaging of 456 hips from 230 adult female volunteers (mean age 66 ± 17 years) was reviewed using 3D multiplanar reformatting to identify bone-related radiological features of osteoarthritis, namely osteophytes, subchondral cysts and joint space narrowing. Scoresheets dividing up the femoral head, head-neck region and the joint space were used to register the location and severity of each feature (scored from 0 to 3). Novel 3D cumulative feature severity maps were then created to display where the most severe disease features from each individual were anatomically located across the cohort.

Results: Feature severity maps showed a propensity for osteophytes at the inferoposterior and superolateral femoral head–neck junction. Subchondral cysts were a less common and less localised phenomenon. Joint space narrowing <1.5 mm was recorded in at least one sector of 83% of hips, but most frequently in the posterolateral joint space.

Conclusions: This is the first description of hip osteoarthritis using unenhanced clinical CT in which we describe the co-localisation of posterior osteophytes and joint space narrowing for the first time. We believe this technique can perform several important roles in future osteoarthritis research, including phenotyping and sensitive disease assessment in 3D.

Introduction

Plain radiographs have been used to diagnose and grade the severity of hip osteoarthritis for more than half a century. Radiographic joint space width (JSW) is currently the only accepted quantitative endpoint measure in early disease modification therapy trials[1], while Kellgren & Lawrence's (K&L) grading has been the preferred method for the assessment of radiological osteoarthritis severity, particularly in clinical and epidemiological research[2–5].

Radiographs are the frontline imaging modality in clinical practice, but they have also allowed researchers to discover patterns of disease in hip osteoarthritis, such as the relationship between osteophyte distribution and femoral head migration[6,7]. Although minimum JSW and K&L grading are associated with an increased risk of total hip replacement (THR)[8], associations between K&L grade and symptomatic osteoarthritis are less clear. Furthermore, K&L grading is based on 2D radiographs that not only introduce geometric distortion but are also unable to fully reflect 3D structure of the hip. This, among other factors, means that interpretation and application of K&L grading can be inconsistent[9], making it a sub-optimal biomarker for disease evaluation.

From a 3D perspective, full topographic representation of the hip can be achieved with cross-sectional magnetic resonance imaging (MRI) and computed tomography (CT). Hayashi *et al.* (2012) have shown that tomosynthesis (a form of radiography that encompasses aspects of 3D information) has better sensitivity for detecting subchondral cysts and osteophytes than plain radiography[10]. The importance of 3D hip and knee assessment in osteoarthritis has been reflected in the development of several semi-quantitative MRI scoring systems. These have most frequently been applied to the knee[11–14], but one has been created for the hip,

* Address correspondence and reprint requests to: T.D. Turmezei, Department of Engineering, University of Cambridge, Trumpington Street, Cambridge CB2 1PZ, UK.
E-mail address: tom@diagnosticradiology.eu (T.D. Turmezei).

http://dx.doi.org/10.1016/j.joca.2014.03.007
1063-4584/

called the hip osteoarthritis MRI scoring system (HOAMS)[15]. The HOAMS study showed that MRI is a reliable modality for imaging soft tissue structures such as cartilage, synovium, ligaments and bone marrow lesions. However mineralised features such as osteophytes, subchondral cysts, subchondral bone density are clearly represented in CT on account of excellent definition with this modality[16–18]. This is very much in line with previous rationales that have considered how CT may not only enhance visualisation of such "cardinal signs" of osteoarthritis, but also how it may contribute to our understanding of the disease[19,20]. Arden *et al.* (2009) have also recommended that researchers consider femoral osteophytes and JSW when defining incident radiographic hip osteoarthritis[21], both features that can be visualised and recorded with CT in detail.

This is the first of two papers that considers the assessment of hip osteoarthritis with unenhanced clinical CT. Here we present a new descriptive technique for mapping the severity and spatial distribution of features associated with hip osteoarthritis in 3D from multiplanar reformats of clinically acquired CT data. We present the cumulative results from our cohort of female volunteers using novel 3D-based feature severity maps.

Methods

Demographics

This study was performed using clinical CT examinations acquired from female volunteers acting as control participants in existing Cambridge trials investigating hip fracture risk from cortical bone thickness measurements. All participants were free of hip fracture, metastatic bone disease, and unilateral metabolic bone disease. Each had given informed consent for analysis of their hip and pelvic imaging data. No clinical information was recorded on the clinical assessment of osteoarthritis or related symptoms such as hip pain or reduced mobility. CT examinations were reported by a consultant radiologist as part of the routine clinical care of patients involved in Cambridge studies (FEMCO: LREC 07-H0305-61; MRC-Hip fx and MRC-Ageing: LREC 06/Q0108/180; MRC-Stroke: LREC 01/245; ACCT-1: LREC 04/Q0108/257). Imaging of 247 female volunteer control participants was available for review. Seventeen of these were excluded on account of: unilateral hip metalwork causing imaging artefact ($n = 9$); lack of complete demographic data ($n = 5$); excessive image noise ($n = 1$); no image files for a registered trial attendant ($n = 1$); or corrupt imaging data files ($n = 1$). The final combined cohort of 230 females had a mean ± standard deviation age of 66 ± 17 years, ranging from 20 to 95 years. Mean weight of the participants was 69.3 ± 14.2 kg. Imaging of only one hip was available in four individuals, so a total of 456 hips were included in the analysis.

Image acquisition and review

Imaging was acquired helically in the supine position on a range of clinical whole-body multidetector CT machines (Siemens SOMATOM Sensation 16, Siemens SOMATOM Sensation 64, Siemens SOMATOM Definition Flash, Siemens SOMATOM Definition AS+, GE Medical Systems Discovery 690). Reconstructed axial slice thickness ranged from 0.75 to 1.5 mm. Peak kV was 120 kV. When available from the anonymised metadata, recorded exposure ranged from 67 to 274 mAs, varying due to routine use of dose limiting. All acquisitions were processed with a standard smooth-edge body reconstruction kernel. No record of symptoms or clinical assessment of hip osteoarthritis was taken at the time of scanning.

Imaging review was performed on a workstation (Osirix v4.0 32-bit, http://www.osirix-viewer.com/, on a v5, 2 iMac, Apple, Cupertino, http://www.apple.com/) using the 3D MPR function with 200% screen zoom, and fixed window level (1800 HU) and width (500 HU). Axial oblique, sagittal oblique and coronal oblique planes were set to the patient's vertical axis and the axis from the centre of the femoral head to the centre of the femoral neck, with the reviewer free to move around the hip joint in these planes (SI Figs. 1 and 2).

Imaging review was performed by a single radiologist who had completed UK specialist training with musculoskeletal subspecialisation (TT). Imaging data were anonymised for all patient identifiers apart from their trial ID number. All distance measurements were made using electronic callipers provided in the Osirix software.

Scoresheet development

In developing HOAMS, Roemer *et al.* (2011) recognised that the structure of the hip joint and its sector of near spherical articular surface posed significant topographic challenges[15]. Our scoresheet [Fig. 1] was created to record the distribution and severity of disease features around the hip joint with sector divisions of the acetabulum, femoral head, and femoral head–neck junction. Radial divisions every 30° (resulting in 12 subdivisions) were inspired by Stelzeneder *et al.* (2012)[22], circumferential divisions by Alvarez *et al.* (2005)[23]. This provided 24 acetabular sectors (12 medial, 12 lateral); 26 femoral head sectors (12 medial, 12 lateral, 2 foveal); and 24 femoral head–neck junction sectors (12 medial, 12 lateral). Acetabular sectors were grouped into seven relevant joint space zones: superolateral, superomedial, anterior, medial, posteromedial, posterolateral, and inferoposterior. Fig. 2 shows how the scoresheet sectors correlate with 3D location on the acetabulum and femoral head/neck.

While the division of axial oblique, sagittal oblique and coronal oblique planes was consistently represented by fixed MPR tool crosshairs for each hip, subsequent sector divisions in these MPR images were subjectively assessed by the reviewer.

Feature assessment

Imaging assessment focused on three bone-related features of osteoarthritis: (1) osteophytes, (2) subchondral cysts, and (3) JSW. Although a recognised radiographic feature of hip osteoarthritis, subchondral bone sclerosis was not assessed because it was considered too unreliable for subjective assessment based on preliminary study. The full guide for assessing features is included in the Supplementary Information (Si).

(1). Osteophytes

No CT definition for an osteophyte exists and so, based on the characterisation of different stages of osteophyte development by Gelse *et al.* (2003)[24], we derived the following definition:

> *"An osteocartilagenous outgrowth or spur with a bony base and cartilaginous cap arising from the periosteum at the junction between articular cartilage and bone, excluding enthesophytes at the point of ligamentous insertion."*

Osteophyte severity was scored as: 0 = none; 1 = possible; 2 = definite osteophyte ≤5 mm from base to tip; 3 = definite osteophyte >5 mm from base to tip. This score was registered in the appropriate sector. If an osteophyte appeared to occupy more than one sector, then sectors were marked as containing it if >50% occupied (see osteophyte assessment – SI Fig. 3 & Table 1).

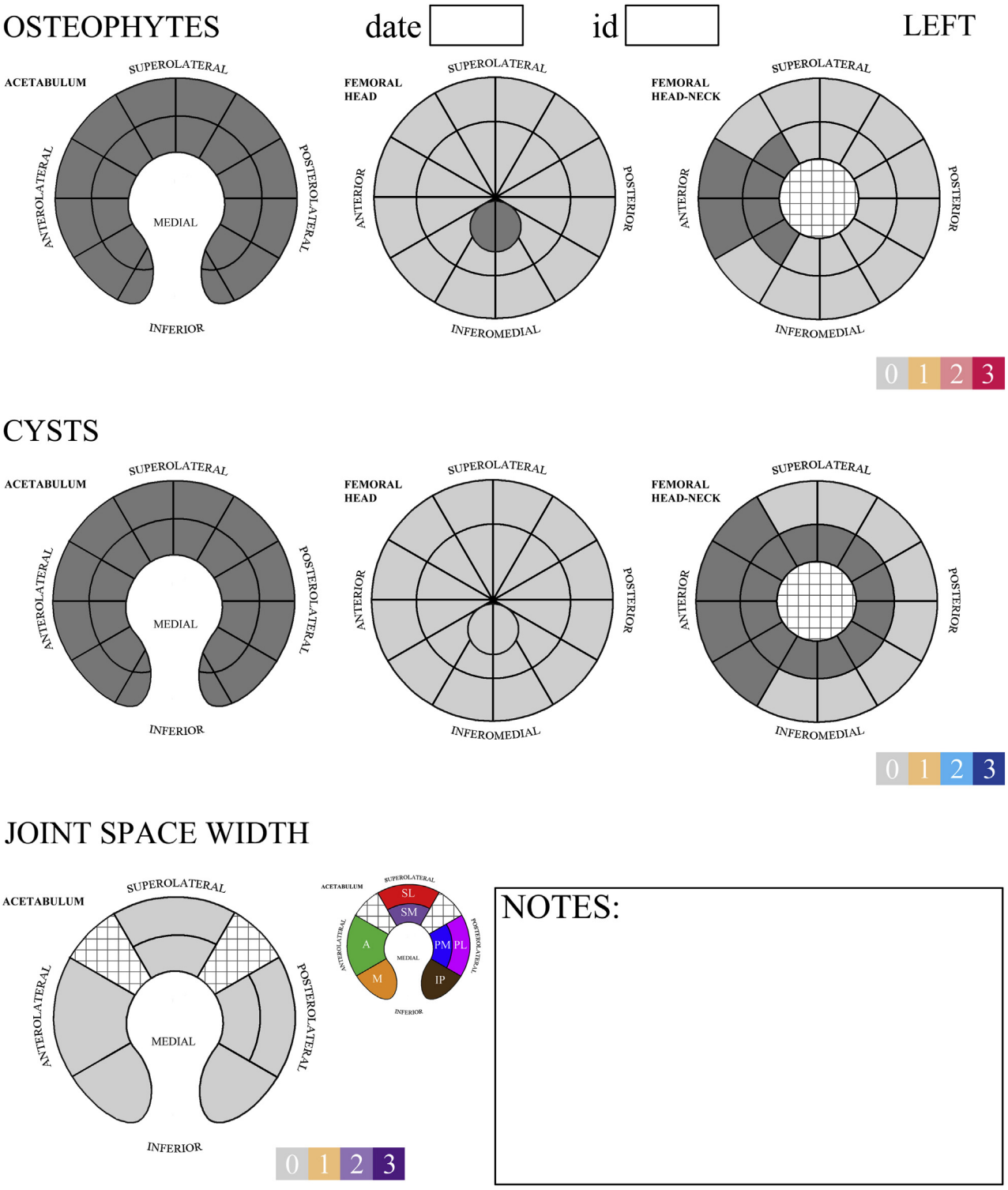

Fig. 1. Scoresheet for assessing bony features of hip osteoarthritis: osteophytes, subchondral cysts and JSW. Cross-hatched areas represent anatomically irrelevant sites (e.g. the femoral neck medulla and non-representative regions of the hip joint space). Dark grey sectors represent those excluded from severity mapping analysis. The reviewer is asked to record if there is bony deformity of the femoral head and can leave additional comment in the 'notes' box. The small inset figure of the acetabulum with each region assigned a different colour is a reminder of the seven the distinct joint space zones, as displayed in Fig. 2.

(2). Subchondral cysts

No assessment of subchondral cyst distribution or severity has been described with clinical CT, however there have been radiographic and CT studies of the proximal femur that have described their appearance[25,26]. Using these reports, with recognition that resolution of clinical CT may limit the detection of overlying cortical breaks, we formulated the following definition for our study:

> *"A low-density region in subchondral bone, usually with a sclerotic rim. Connection with the articular surface need not be visible."*

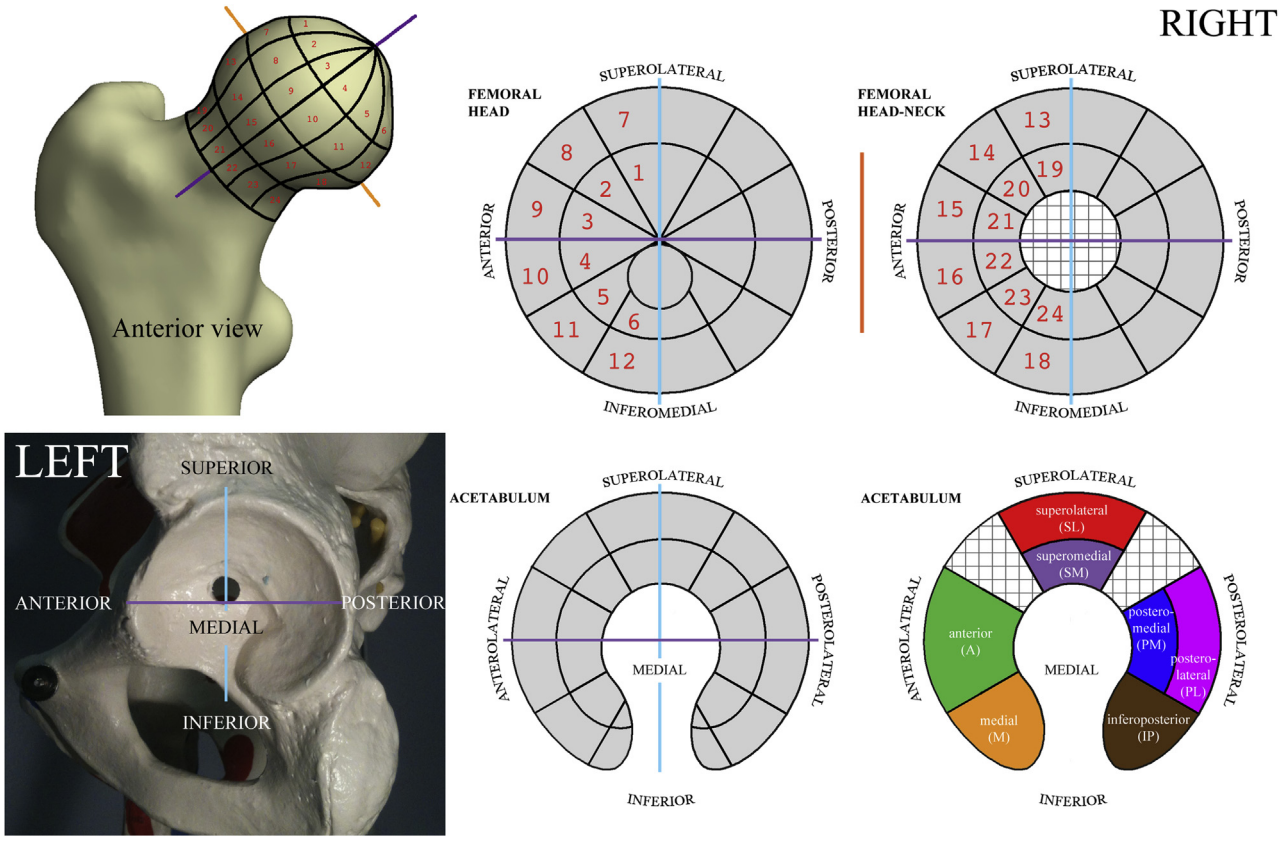

Fig. 2. Sector representations visually correlated between 3D structure and the stylised scoresheet as demonstrated on the right hip and left acetabulum. These sides are chosen for ease of conceptualistaion for the first-time reader. Cross-hatched regions represent anatomically irrelevant sites. **Top row**: Orientation images for the femoral head and neck demonstrated with the anterior view of a right femur. Numbered anterior sectors show how they are represented in a 3D model. The cyan line represents the coronal oblique plane cast through the vertical; the purple line represents the axial oblique plane cast along the long axis from the centre of the femoral head and neck; the orange line represents the orthogonal sagittal oblique plane. **Bottom row**: Orientation images for the acetabulum and resultant joint space zones demonstrated with a lateral the view of the left acetabulum. The cyan line again represents the coronal oblique plane through the vertical; the purple line again represents the axial oblique plane along the long axis from the centre of the femoral head and neck.

Cyst severity was scored as: 0 = none; 1 = possible; 2 = single definite cyst ≤5 mm in maximal diameter; 3 = single definite cyst >5 mm in maximal diameter or multiple cysts ≤5 mm in maximal diameter in the same sector. This score was registered in the appropriate sector. If a cyst occupied more than one sector, then they were all marked as containing it if >50% occupied. If >10 mm cyst was in multiple sectors then occupied sectors were scored 3 (see subchondral cyst assessment – SI Fig. 4 & Table 2).

(3). JSW

Given the limitations of unenhanced clinical CT in defining femoral and acetabular cartilage thickness independently, the surrogate marker of JSW was used. There have been several measures of JSW applied to radiographs but not for manual measurement in CT. We decided to divide JSW categories according to Croft *et al.* (1990) with an arbitrary lower limit of normal chosen at 4.5 mm[27]. The narrowest distance measured from cortical surface to cortical surface with electronic calipers was recorded in predetermined zones [Fig. 2], including any cortical bony protrusion or osteophyte. JSW within any given sector was thus scored as: 0 = ≥4.5 mm; 1 = ≥2.5–4.5 mm; 2 = ≥1.5–2.5 mm; 3 = <1.5 mm (see JSW assessment – SI Figs. 1 & 2).

Adobe Photoshop CS4 v11.0.2 (Adobe Systems Inc., www.adobe.com.uk) was used to create and fill the scoresheets and severity maps. It took less than 5 min to grade a single hip with severe disease using the methods described.

Feature severity mapping

In order to visualise the most frequent anatomical location of hip osteoarthritis features across the cohort, we devised a new technique of data presentation called 'feature severity mapping'. The purpose of feature severity mapping is to give a 3D visual representation of where most severe features are located in a cohort, identifying the most likely location of a given disease feature by using a colour proportion scale. If features coincide at specific anatomical locations and different severities, then this might give useful information on the evolution of disease.

An empty 'cumulative' scoresheet was prepared for scores of 1, 2 and 3 for each of osteophytes, subchondral cysts and JSW. Original assessment scoresheets were then reviewed in turn for each of the 456 femurs in the cohort. The anatomical sector containing the most severe score for each feature was identified and the count increased by one in this sector on the appropriate cumulative

Table I
Frequency of most severe feature score for each hip (n_{total})

	Frequency of most severe feature score, n_{total} (%)				
Feature	0	1	2	3	Total
Osteophyte	82 (18)	136 (29.8)	209 (45.8)	29 (6.4)	456 (100)
Cyst	348 (76.3)	36 (7.9)	40 (8.8)	32 (7)	456 (100)
JSW	0 (0)	1 (0.2)	77 (16.9)	378 (82.9)	456 (100)

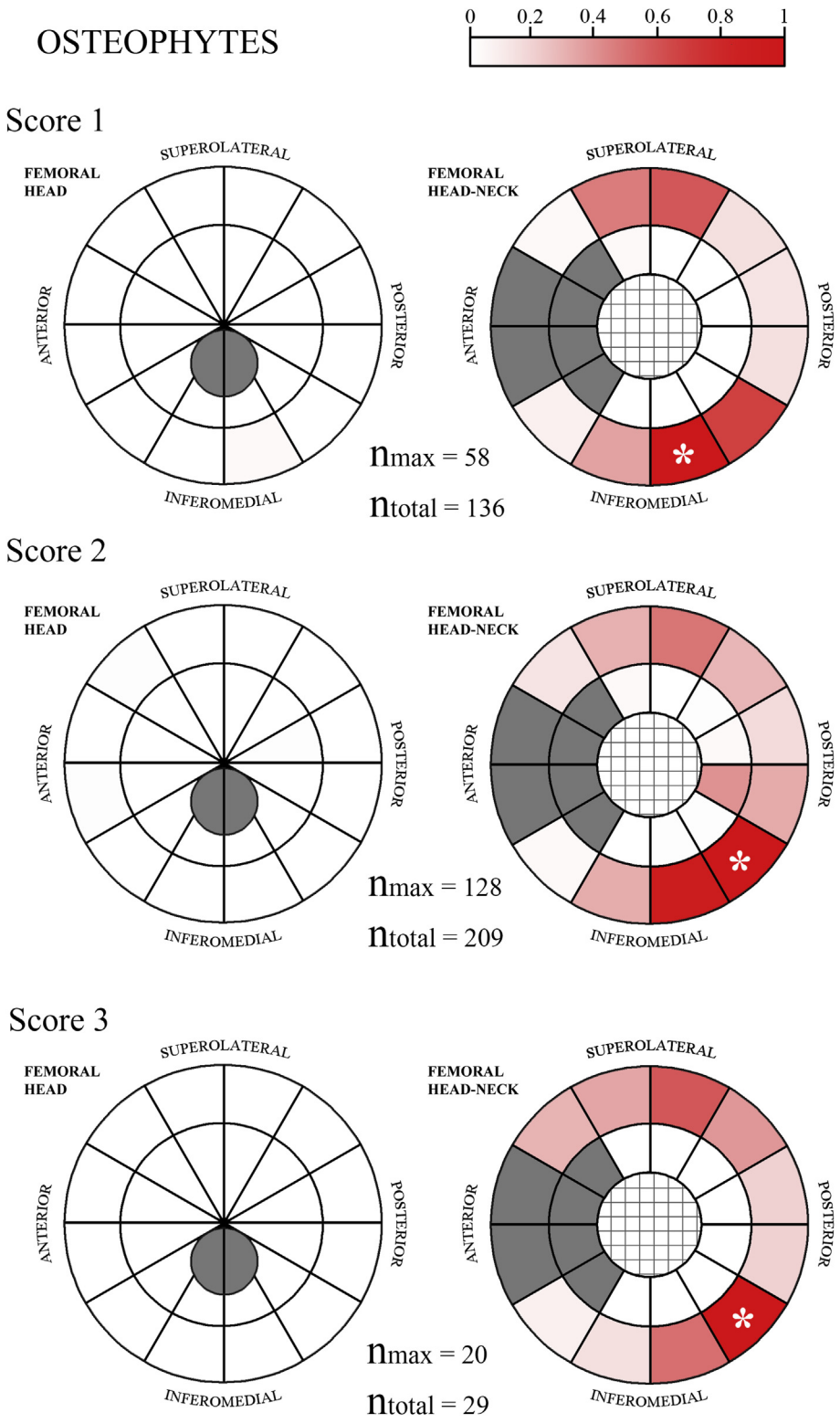

Fig. 3. 2D feature severity maps for osteophytes represented on the stylised scoresheets with excluded sectors in grey. Features of a given score appeared most often in the sector coloured with deepest shade of red (the n_{max} sector, labelled with *), with the remaining sectors for that score shaded proportionally according to the colour scale.

scoresheet. If worst scores were equal across sectors, then the count was increased by one in each sector. This method assumed linearity in the original feature scoring (from 0 to 3) and in the increasing cumulative score counts. The process was repeated for each hip in the cohort. The cumulative count in each sector was then calculated as a proportion of the number of counts in the highest scoring sector for the given feature score, called the ***n*max sector**. Proportions were represented as a colour scale (osteophytes = red, cysts = blue, JSW = purple) using the darkest shade for the n_{max} sector, increasing in brightness to white for a proportion of zero.

Results for osteophytes and cysts were also translated onto a 3D surface of the proximal femur, with JSW results presented on a stylised 2D scoresheet map. We recorded the total number of hips whose most severe feature score was 0, 1, 2 and 3 respectively, calling this number $\boldsymbol{n_{total}}$.

There were several exclusion zones for this exercise (featured as dark grey sectors in Fig. 1):

- 'Osteophytes' around the fovea, which were considered to be enthesophytes;
- 'Osteophytes' at the anterior femoral neck and head–neck junction, which were considered to be a reaction area rather than a true osteophyte[28];
- 'Cysts' at the anterior femoral neck and head–neck junction, which were considered to be a herniation pit[28];
- 'Cysts' circumferentially around the femoral neck where not beneath articular cartilage, which were considered to be herniation pit variants; and
- All features around the acetabulum, because of indeterminacy between an acetabular osteophyte vs acetabular lipping or labral calcification and whether a low-density lesion in the acetabular rim was a true subchondral cyst or an invading labral cyst. Excluding the acetabulum also significantly reduced the time for image analysis.

Results

Frequency of features

The frequencies of the most severe disease feature scores from across the cohort (n_{total}) are given in Table I. Although these provide an overview of feature prevalence, this loses the topographic 3D information obtained from imaging assessment, hence the creation of feature severity maps to show their sector distribution.

Osteophytes

There were 136 hips ($n_{total} = 136$) with an osteophyte score of 1 as most severe; 58 of these (43%) were in the n_{max} sector. There were 209 hips with an osteophyte score of 2 as most severe; 128 of these (61%) were in the n_{max} sector. There were 29 hips with an osteophyte score of 3 as the most severe; 20 of these (69%) were in the n_{max} sector. There were an additional 82 hips free of osteophytes (not shown). See Fig. 3 for a 2D visual representation of these results on the stylised scoresheet sectors and Fig. 4 for the same results represented in 3D on a canonical femur.

Subchondral cysts

There were 36 hips with a cyst score of 1 as most severe ($n_{total} = 36$); 5 of these (14%) were in the n_{max} sector. There were 40 hips with a severest cyst score of two ($n_{total} = 40$); 6 of these (15%) were in the n_{max} sector. There were 32 hips with a cyst score of 3 as most severe ($n_{total} = 32$); 5 of these (16%) were in the n_{max} sector. There were an additional 348 hips free of cysts (not shown). See Fig. 5 for a 2D visual representation of these results on the stylised scoresheet sectors and Fig. 6 for the same results represented in 3D on a canonical femur.

JSW

Only 1 hip had a most severe feature score of 1, with this score in every joint space zone (n_{total} and $n_{max} = 1$). There were 77 hips with a JSW score of 2 as most severe ($n_{total} = 77$); 61 of these (79%) were in the n_{max} sector. Similarly, there were 378 hips with a JSW score of 3 as most severe ($n_{total} = 378$); 280 of these (74%) were in the n_{max} sector. No hips had a score of 0 across all sectors. See Fig. 7 for a visual representation of these results on the stylised 2D scoresheet sectors.

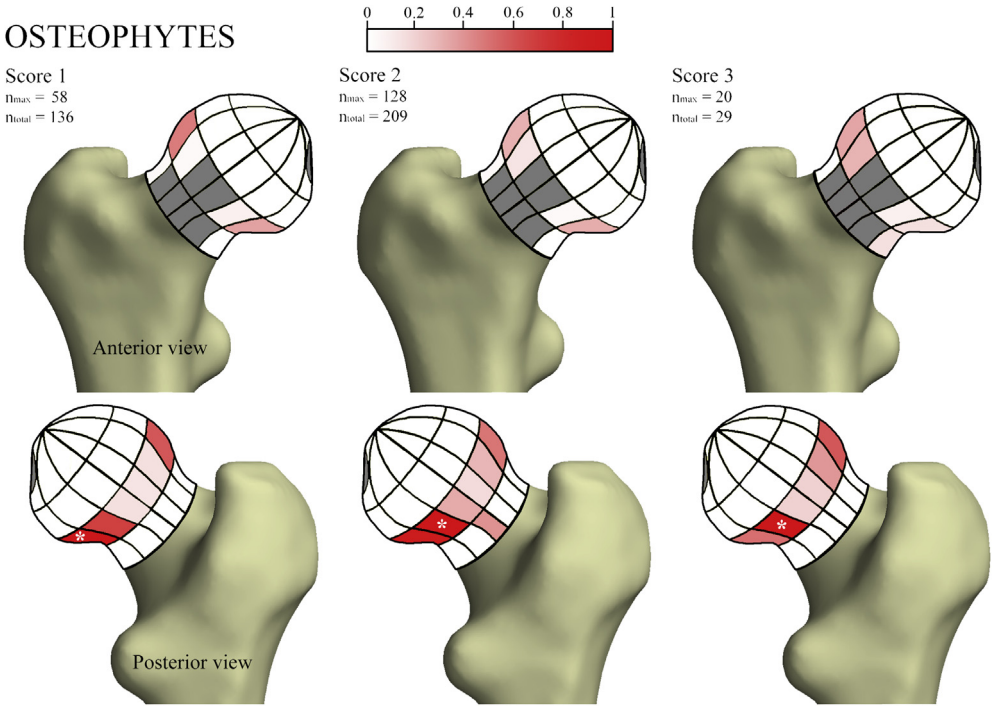

Fig. 4. 3D feature severity maps for osteophytes represented on a canonical right femur model with excluded sectors in grey. Features of a given score appeared most often in the sector coloured with deepest shade of red (the n_{max} sector, labelled *), with the remaining sectors for that score shaded proportionally according to the colour scale.

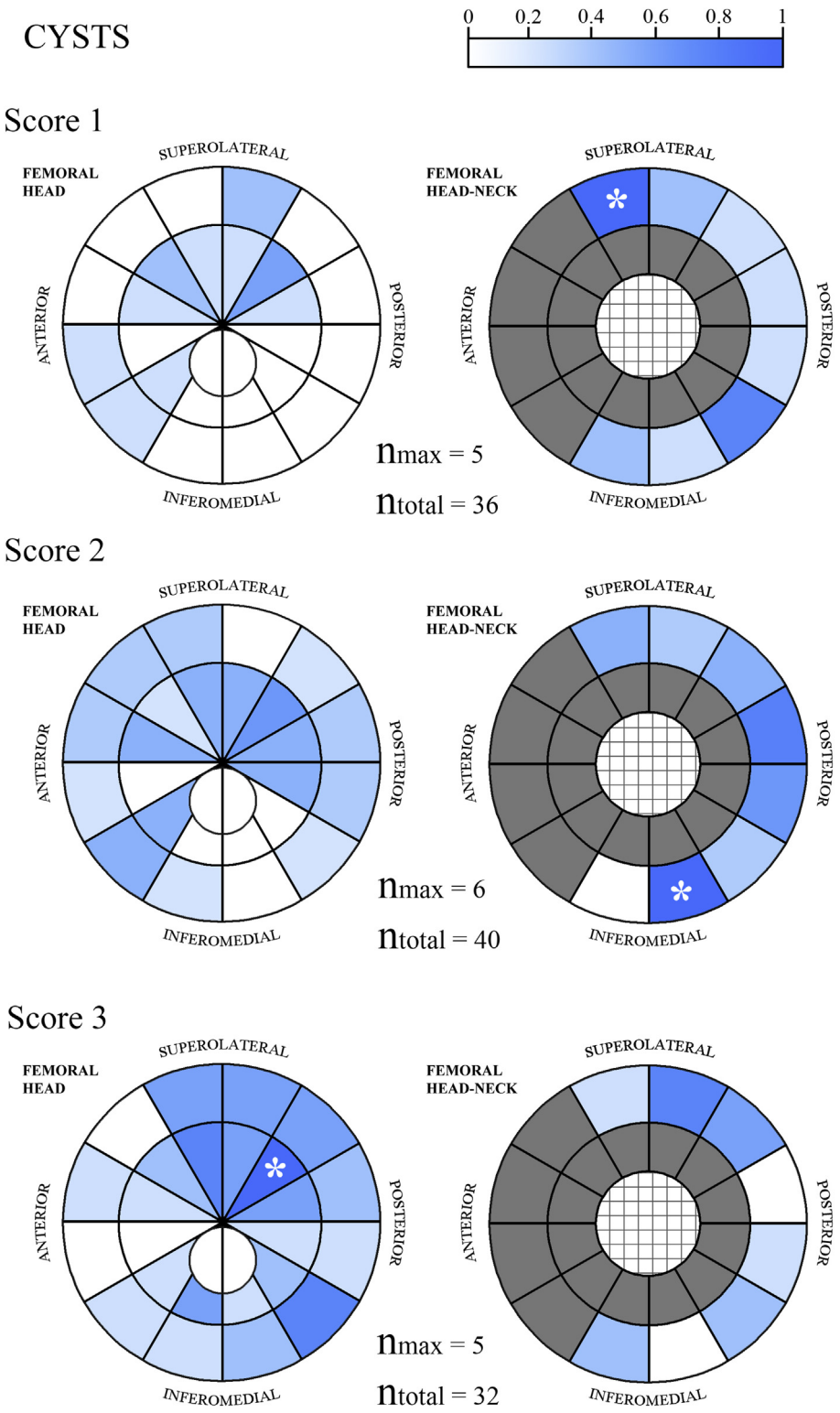

Fig. 5. 2D feature severity maps for subchondral cysts represented on the stylised scoresheets with excluded sectors in grey. Features of a given score appeared most often in the sector coloured with deepest shade of blue (the n_{max} sector, labelled *), with the remaining sectors for that score shaded proportionally according to the colour scale.

Discussion

CT has not been a popular choice for the assessment of osteoarthritis. Despite its widespread availability and early promise as a diagnostic tool[29], recent reviews have overlooked the technique, focussing instead on MRI[30–33]. In June 2011, Hunter and Eckstein reported on quantitative CT (QCT) assessment of bone mineral density in knee osteoarthritis in conference proceedings[34], while Bousson *et al.* (2012) have developed the Medical Image Analysis Framework born from osteoporosis assessment for application in osteoarthritis at the knee[19]. Nonetheless, published CT methods are rare compared to those that feature radiography and/or MRI.

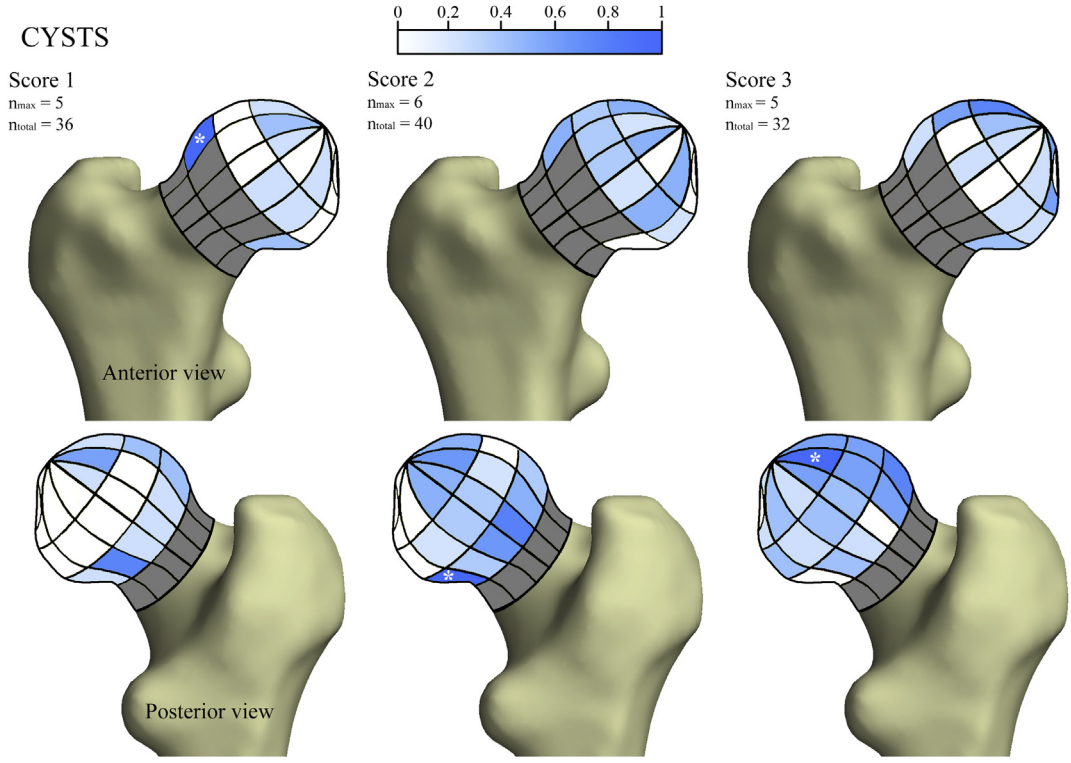

Fig. 6. 3D feature severity maps for subchondral cysts represented on a right canonical femur model with excluded sectors in grey. Features of a given score appeared most often in the sector coloured with deepest shade of blue (the n_{max} sector, labelled *), with the remaining sectors for that score shaded proportionally according to the colour scale.

Reasons for this include the higher radiation dose of CT compared to radiography and its inability to show cartilage damage in the absence of intra-articular contrast medium. CT arthrography (requiring an invasive intra-articular injection to induce contrast between bone, articular cartilage and the joint space) has been studied in relation to osteoarthritis[23], but finds little clinical application outside of patients in whom MRI is contraindicated. Contrast-enhanced peripheral quantitative CT has been used as a research tool in the assessment of proteoglycan content of articular cartilage in much the same way as dGEMRIC (delayed gadolinium enhanced MRI of cartilage), but has only been published as an *in vitro* research method[35].

In this first of two papers on unenhanced clinical CT assessment of hip osteoarthritis, our new technique of feature severity mapping has been able to demonstrate the 3D distribution of disease features around the proximal femur and hip joint space in a cohort of adult women. The most frequent location of osteophytes was at the inferoposterior femoral head–neck junction across all scores [Figs. 3 and 4], a site partially obscured in anteroposterior (AP) radiographs but considered important for correct hip joint alignment[36] and often encountered at hip arthroscopy where they are considered difficult to reach and a challenge to remove[37]. Osteophytes were also frequently recorded at the superolateral femoral head–neck junction across all scores [Figs. 3 and 4], a finding that could be explained by reaction to impingement with the adjacent osseous acetabulum or fibrocartilagenous labrum[38]. These features are in a recognised distribution of a marginal peri-articular osteophytic process. Subarticular and epi-articular osteophytes were rare in this cohort, even as an extension of the peri-articular osteophytes seen in severe disease[39].

The overall frequency of subchondral cysts was low compared to osteophytes (definite in 15.8% vs 52.2%). Feature severity mapping showed no pattern to their distribution, but severe subchondral cysts were most frequent in the superior weight-bearing surface of the femoral head [Figs. 5 and 6]. The presence of single subcortical cysts at different sites around the femoral head–neck junction suggests that they may be from a similar phenomenon to the anterosuperior herniation pit[28], but at a different site (SI Fig. 5). The relationship of subcortical pits with hip biomechanics and joint degeneration is yet to be understood.

There have been cadaveric studies that have mapped the 3D distribution of acetabular cartilage thickness using CT arthrography[40,41] and contact-type 3D digitization[42], but until now no CT technique had approached the entity of hip JSW *in vivo*. We report two important JSW findings. Firstly, minimum JSW was less than 2.5 mm in 99.8% and less than 1.5 mm in 82.9% of hips. Even though a record of symptomatic disease was not taken, it seems unlikely that all hips meeting JSW thresholds set by Croft *et al.* (1990) should have cartilage damage[27]. This could be explained by possible dependent behaviour of cartilage (i.e., being compressed by physical pressure in the supine position to narrow inter-bone distance), or by the fact that we do not yet know the threshold for 'normal' CT-recorded JSW. The former could be answered by comparing JSW between supine and prone acquisitions in the same individual, although one literature review reported on a study that showed no difference in JSW between pelvic radiographs taken supine and standing[43]. The latter could be answered by correlating sites and severity of joint space narrowing with symptomatic disease. Secondly, we identified a propensity for narrowest joint space to be at the posterior aspect [Fig. 7]. This co-localises with the finding of thinnest cartilage in the posterior aspect of the acetabulum as demonstrated by a digitized proximity mapping technique in cadaveric specimens[42]. There is also a visual concordance of JSW $<$1.5 mm and osteophytes at all scores at the posterolateral and inferoposterior aspect of the hip joint. This region is partially obscured in conventional AP radiographs, so more needs to be

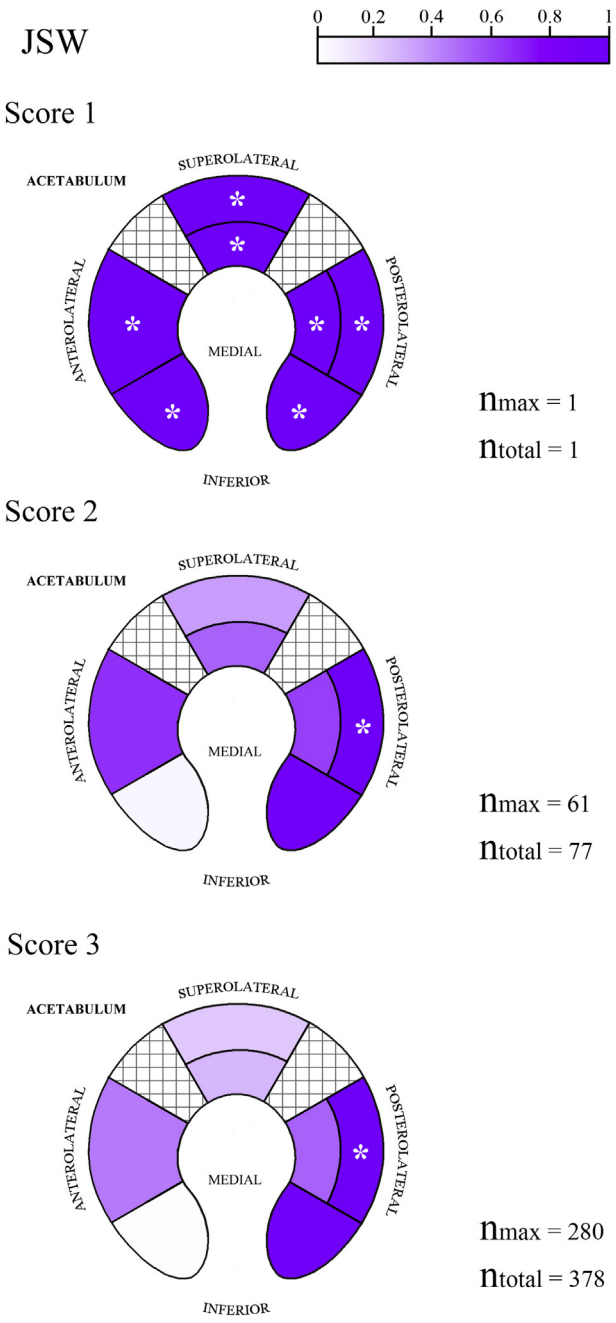

Fig. 7. Feature severity maps for JSW represented in the 2D stylised joint zones. Features of a given score appeared most often in the sector coloured with deepest shade of purple (the n_{max} sector, labelled *), with the remaining sectors for that score shaded proportionally according to the colour scale.

understood about why features of disease are so prevalent here. The skewed distribution of JSW towards values less than 2.5 mm (99.8% of hips) demonstrates that further study with CT will also need to redress category division boundaries to allow for discrimination of smaller JSWs in a study population.

Limitations

We recognise that imaging features have not been correlated with clinical symptoms such as pain and reduced function, the former of which is still poorly understood in relation to structural disease[44]. There will also be an overlap between normal ageing and osteoarthritis because the prevalence of symptomatic and radiological hip disease both increase with age[45], meaning that they cannot be separated from an aetiological perspective. We are now conducting a follow-on study that will correlate THR as a clinical determinant of disease with radiological features in a cohort with baseline and 5-year follow-up CT imaging, and investigate disease pattern in males.

We also recognise that radiographic JSW can vary within the hip joint[46], raising the question of where JSW measurements should be made. Errors introduced by manual MPR alignment and electronic caliper measurements in the assessment process must also be considered. Given that results are presented here as the output of a descriptive study, these factors have not introduced numerical error into significance testing, and so can be considered consistent across all measurements. However, they are discussed in full detail in our next paper in relation to the development and reliability testing of a new CT grading system for hip osteoarthritis, which we also compare against a gold standard of K&L grading of radiographs digitally reconstructed from the same CT data[50].

This has been an important first step in CT assessment of radiological features that are associated large joint osteoarthritis, especially since one cohort study involving nearly 3,000 participants with a 2.5% THR rate has already shown that the presence of radiographic osteoarthritis is strongly linked with future replacement, regardless of symptoms[8]. We believe that reliance on radiography may be missing important structural features of disease such as the collocated posterior osteophytes and joint space narrowing that we have been able to demonstrate with CT.

Applications

There are several important potential roles for CT-based feature severity mapping. With the application of appropriate statistical testing such as statistical parametric mapping[47], individual scoresheets and cohort severity maps could be compared with those at follow-up in clinical trials or epidemiological studies to assess changes in feature severity and distribution. They could be applied in a cohort of symptomatic and asymptomatic volunteers to address how much aging and other risk factors are responsible for imaging features. They also have the capability to inform us about thumbprints of different disease phenotypes (for example, developing on the concept of atrophic vs hypertrophic disease[6,7]) and their significance in onset, progression and response to therapy for hip osteoarthritis. The outcome of such work would be instrumental for genetic and therapeutic studies[48]. It is likely that radiographic imaging has not been able to establish phenotypes accurately enough to yield the most from the current wave of genetic studies, and so the ability of CT to define these features more accurately needs consideration.

Finally, a recent study by Felson *et al.* (2013) suggested that osteoarthritis of the knee was a disease with inertia, though radiographs were precarious in the veracity with which they were able to represent disease at different time points[49]. The application of feature severity mapping using multiplanar CT image reconstruction would remove such variability, including positional and geometric distortion factors that can confound radiographic disease assessment.

Conclusion

This study has reported on feature severity mapping, a new descriptive technique for 3D assessment of imaging features of hip osteoarthritis from unenhanced clinical CT. We have identified that the inferoposterior and posterolateral hip joint are important sites

of osteophyte and JSW collocation. This region is poorly represented in AP radiographs and so more needs to be understood about how and why radiological features of disease are prevalent here. The superolateral femoral head–neck junction is also an important site of osteophyte development in a location that suggests it could be related to impingement phenomena. Finally, we believe that feature severity mapping has the potential to develop in several important roles for the assessment of hip osteoarthritis, including phenotyping and sensitive 3D disease representation. We take this work forward with our follow-up paper on the development and reliability testing of a new CT grading for hip osteoarthritis[50].

Contributions

TT, DL, MH and KP contributed to conception and design of this study.

TT performed data collection.

TT, DL and KP conducted data analysis.

TT, DL, MH, and KP contributed to data interpretation and preparation of the manuscript. The final version of the article was approved by all the authors.

TT takes responsibility for the integrity of the work as a whole.

Competing interests

None declared.

Funding sources

KP acknowledges support of an Arthritis Research UK Research Progression award, and the Cambridge NIHR Biomedical Research Centre (MEBB theme). TT acknowledges the support of an Evelyn Trust Clinical Training Fellowship award. None of the funding sources had a role in study design, data handling, writing of the report, or decision to submit the paper for publication.

Acknowledgements

None.

Supplementary data

Supplementary data related to this article can be found at http://dx.doi.org/10.1016/j.joca.2014.03.007.

References

1. Hunter DJ, Eckstein F, Kraus VB, Losina E, Sandell L, Guermazi A. Imaging biomarker validation and qualification report: sixth OARSI workshop on imaging in osteoarthritis combined with third OA biomarkers workshop. Osteoarthritis Cartilage 2013;21:939–42.
2. Altman RD, Gold GE. Atlas of individual radiographic features in osteoarthritis, revised. Osteoarthritis Cartilage 2007;15(Suppl A):A1–56.
3. Kellgren JH, Lawrence JS. Radiological assessment of osteo-arthrosis. Ann Rheum Dis 1957;16:494–502.
4. Reijman M, Hazes JM, Koes BW, Verhagen AP, Bierma-Zeinstra SM. Validity, reliability, and applicability of seven definitions of hip osteoarthritis used in epidemiological studies: a systematic appraisal. Ann Rheum Dis 2004;63:226–32.
5. Ornetti P, Brandt K, Hellio-Le Graverand MP, Hochberg M, Hunter DJ, Kloppenburg M, *et al*. OARSI-OMERACT definition of relevant radiological progression in hip/knee osteoarthritis. Osteoarthritis Cartilage 2009;17:856–63.
6. Ledingham J, Dawson S, Preston B, Milligan G, Doherty M. Radiographic patterns and associations of osteoarthritis of the hip. Ann Rheum Dis 1992;51:1111–6.
7. Solomon L, Schnitzler CM, Browett JP. Osteoarthritis of the hip: the patient behind the disease. Ann Rheum Dis 1982;41(2):118–25.
8. Franklin J, Ingvarsson T, Englund M, Ingimarsson O, Robertsson O, Lohmander LS. Natural history of radiographic hip osteoarthritis: a retrospective cohort study with 11-28 years of followup. Arthritis Care Res (Hoboken) 2011;63(5):689–95.
9. Schiphof D, Boers M, Bierma-Zeinstra SM. Differences in descriptions of Kellgren and Lawrence grades of knee osteoarthritis. Ann Rheum Dis 2008;67(7):1034–6.
10. Hayashi D, Xu L, Roemer FW, Hunter DJ, Li L, Katur AM, *et al*. Detection of osteophytes and subchondral cysts in the knee with use of tomosynthesis. Radiology 2012;263(1):206–15.
11. Peterfy CG, Guermazi A, Zaim S, Tirman PF, Miaux Y, White D, *et al*. Whole-Organ Magnetic Resonance Imaging Score (WORMS) of the knee in osteoarthritis. Osteoarthritis Cartilage 2004;12(3):177–90.
12. Hunter DJ, Lo GH, Gale D, Grainger AJ, Guermazi A, Conaghan PG. The reliability of a new scoring system for knee osteoarthritis MRI and the validity of bone marrow lesion assessment: BLOKS (Boston Leeds Osteoarthritis Knee Score). Ann Rheum Dis 2008;67(2):206–11.
13. Kornaat PR, Ceulemans RY, Kroon HM, Riyazi N, Kloppenburg M, Carter WO, *et al*. MRI assessment of knee osteoarthritis: Knee Osteoarthritis Scoring System (KOSS)–inter-observer and intra-observer reproducibility of a compartment-based scoring system. Skelet Radiol 2005;34(2):95–102.
14. Hunter DJ, Guermazi A, Lo GH, Grainger AJ, Conaghan PG, Boudreau RM, *et al*. Evolution of semi-quantitative whole joint assessment of knee OA: MOAKS (MRI Osteoarthritis Knee Score). Osteoarthritis Cartilage 2011;19(8):990–1002.
15. Roemer FW, Hunter DJ, Winterstein A, Li L, Kim YJ, Cibere J, *et al*. Hip Osteoarthritis MRI Scoring System (HOAMS): reliability and associations with radiographic and clinical findings. Osteoarthritis Cartilage 2011;19(8):946–62.
16. Lim YW, van Riet RP, Mittal R, Bain GI. Pattern of osteophyte distribution in primary osteoarthritis of the elbow. J Shoulder Elb Surg 2008;17(6):963–6.
17. McErlain DD, Milner JS, Ivanov TG, Jencikova-Celerin L, Pollmann SI, Holdsworth DW. Subchondral cysts create increased intra-osseous stress in early knee OA: a finite element analysis using simulated lesions. Bone 2011;48(3):639–46.
18. Chiba K, Ito M, Osaki M, Uetani M, Shindo H. In vivo structural analysis of subchondral trabecular bone in osteoarthritis of the hip using multi-detector row CT. Osteoarthritis Cartilage 2011;19(2):180–5.
19. Bousson V, Lowitz T, Laouisset L, Engelke K, Laredo JD. CT imaging for the investigation of subchondral bone in knee osteoarthritis. Osteoporos Int 2012;23:S861–5.
20. Turmezei TD, Poole KE. Computed tomography of subchondral bone and osteophytes in hip osteoarthritis: the shape of things to come? Front Endocrinol (Lausanne) 2011:297.
21. Arden NK, Lane NE, Parimi N, Javaid KM, Lui LY, Hochberg MC, *et al*. Defining incident radiographic hip osteoarthritis for epidemiologic studies in women. Arthritis Rheum 2009;60(4):1052–9.
22. Stelzeneder D, Mamisch TC, Kress I, Domayer SE, Werlen S, Bixby SD, *et al*. Patterns of joint damage seen on MRI in early hip osteoarthritis due to structural hip deformities. Osteoarthritis Cartilage 2012;20(7):661–9.

23. Alvarez C, Chicheportiche V, Lequesne M, Vicaut E, Laredo JD. Contribution of helical computed tomography to the evaluation of early hip osteoarthritis: a study in 18 patients. Jt Bone Spine 2005;72(6):578–84.
24. Gelse K, Söder S, Eger W, Diemtar T, Aigner T. Osteophyte development–molecular characterization of differentiation stages. Osteoarthritis Cartilage 2003;11(2):141–8.
25. Resnick D, Niwayama G, Coutts RD. Subchondral cysts (geodes) in arthritic disorders: pathologic and radiographic appearance of the hip joint. Am J Roentgenol 1977;128(5):799–806.
26. Panzer S, Esch U, Abdulazim AN, Augat P. Herniation pits and cystic-appearing lesions at the anterior femoral neck: an anatomical study by MSCT and μCT. Skelet Radiol 2010;39(7):645–54.
27. Croft P, Cooper C, Wickham C, Coggon D. Defining osteoarthritis of the hip for epidemiologic studies. Am J Epidemiol 1990;132(3):514–22.
28. Pitt MJ, Graham AR, Shipman JH, Birkby W. Herniation pit of the femoral neck. Am J Roentgenol 1982;138(6):1115–21.
29. Chan WP, Lang P, Stevens MP, Sack K, Majumdar S, Stoller DW, *et al*. Osteoarthritis of the knee: comparison of radiography, CT, and MR imaging to assess extent and severity. Am J Roentgenol 1991;157(4):799–806.
30. Braun HJ, Gold GE. Diagnosis of osteoarthritis: imaging. Bone 2012;51(2):278–88.
31. Hunter DJ. Advanced imaging in osteoarthritis. Bull NYU Hosp Jt Dis 2008;66(3):251–60.
32. Hayashi D, Roemer FW, Guermazi A. Osteoarthritis year 2011 in review: imaging in OA–a radiologists' perspective. Osteoarthritis Cartilage 2012;20(3):207–14.
33. Roemer FW, Crema MD, Trattnig S, Guermazi A. Advances in imaging of osteoarthritis and cartilage. Radiology 2011;260(2):332–54.
34. Hunter DJ, Eckstein F. From joint anatomy to clinical outcomes in osteoarthritis and cartilage repair: summary of the fifth annual osteoarthritis imaging workshop. Osteoarthritis Cartilage 2011;19(11):1263–9.
35. Kallioniemi AS, Jurvelin JS, Nieminen MT, Lammi MJ, Töyräs J. Contrast agent enhanced pQCT of articular cartilage. Phys Med Biol 2007;52(4):1209–19.
36. Mitsui H, Iguchi I, Kobayashi K, Nagaya Y, Goto H, Nozaki M, *et al*. Self Compensation of excessive Anteversion by osteophytes in hip arthritis. Bone Jt J 2013;95-B(Suppl 15):264.
37. Byrd JWT. Decision making in osteoarthritis. In: Byrd JWT, Ed. Operative Hip Arthroscopy. New York: Springer; 2012:263–78.
38. Ganz R, Leunig M, Leunig-Ganz K, Harris WH. The etiology of osteoarthritis of the hip: an integrated mechanical concept. Clin Orthop Relat Res 2008;466(2):264–72.
39. Jeffery AK. Osteophytes and the osteoarthritic femoral head. J Bone Jt Surg Br 1975;57(3):314–24.
40. Wyler A, Bousson V, Bergot C, Polivka M, Leveque E, Vicaut E, *et al*. Hyaline cartilage thickness in radiographically normal cadaveric hips: comparison of spiral CT arthrographic and macroscopic measurements. Radiology 2007;242(2):441–9.
41. Allen BC, Peters CL, Brown NA, Anderson AE. Acetabular cartilage thickness: accuracy of three-dimensional reconstructions from multidetector CT arthrograms in a cadaver study. Radiology 2010;255(2):544–52.
42. Akiyama K, Sakai T, Koyanagi J, Murase T, Yoshikawa H, Sugamoto K. Three-dimensional distribution of articular cartilage thickness in the elderly cadaveric acetabulum: a new method using three-dimensional digitizer and CT. Osteoarthritis Cartilage 2010;18(6):795–802.
43. Altman RD, Bloch DA, Dougados M, Hochberg M, Lohmander S, Pavelka K, *et al*. Measurement of structural progression in osteoarthritis of the hip: the Barcelona consensus group. Osteoarthritis Cartilage 2004;12(7):515–24.
44. Hunter DJ, Guermazi A, Roemer F, Zhang Y, Neogi T. Structural correlates of pain in joints with osteoarthritis. Osteoarthritis Cartilage 2013;21(9):1170–8.
45. Guillemin F, Rat AC, Mazieres B, Pouchot J, Fautrel B, Euller-Ziegler L, *et al*. Prevalence of symptomatic hip and knee osteoarthritis: a two-phase population-based survey. Osteoarthritis Cartilage 2011;19(11):1314–22.
46. Lequesne M, Malghem J, Dion E. The normal hip joint space: variations in width, shape, and architecture on 223 pelvic radiographs. Ann Rheum Dis 2004, Sep;63(9):1145–51.
47. Friston KJ, Holmes AP, Worsley KJ, Poline JP, Frith CD, Frackowiak RSJ. Statistical parametric maps in functional imaging: a general linear approach. Hum Brain Mapp 1994;2(4):189–210.
48. Lanyon P, Muir K, Doherty S, Doherty M. Influence of radiographic phenotype on risk of hip osteoarthritis within families. Ann Rheum Dis 2004;63(3):259–63.
49. Felson D, Niu J, Sack B, Aliabadi P, McCullough C, Nevitt MC. Progression of osteoarthritis as a state of inertia. Ann Rheum Dis 2013;72(6):924–9.
50. Turmezei TD, Fotiadou A, Lomas DJ, Hopper MA, Poole KE. A new CT grading system for hip osteoarthritis. Osteoarthritis Cartilage 2014;22(10):1360–6.